

Paramagnetism of the Co sublattice in ferromagnetic $\text{Zn}_{1-x}\text{Co}_x\text{O}$ films

A. Barla,^{1,*} G. Schmerber,¹ E. Beaurepaire,¹ A. Dinia,¹ H. Bieber,¹ S. Colis,¹ F. Scheurer,¹ J.-P. Kappler,¹ P. Imperia,² F. Nolting,³ F. Wilhelm,⁴ A. Rogalev,⁴ D. Müller,⁵ and J. J. Grob⁵

¹*Institut de Physique et Chimie des Matériaux de Strasbourg, UMR 7504 ULP-CNRS, 23 rue du Loess, BP 43, F-67034 Strasbourg Cedex 2, France*

²*Hahn Meitner Institut, Glienicker Strasse 100, D-14109 Berlin, Germany*

³*Swiss Light Source, Paul Scherrer Institut, CH-5232 Villigen PSI, Switzerland*

⁴*European Synchrotron Radiation Facility, Boîte Postale 220, F-38043 Grenoble Cedex 9, France*

⁵*InESS, UMR 7163 CNRS, 23 rue du Loess, Boîte Postale 20CR, F-67037 Strasbourg Cedex 2, France*

(Received 7 December 2006; revised manuscript received 9 May 2007; published 4 September 2007)

Using the spectroscopies based on x-ray absorption, we have studied the structural and magnetic properties of $\text{Zn}_{1-x}\text{Co}_x\text{O}$ films ($x=0.1$ and 0.25) produced by reactive magnetron sputtering. These films show ferromagnetism with a Curie temperature T_C above room temperature in bulk magnetization measurements. Our results show that the Co atoms are in a divalent state and in tetrahedral coordination, thus substituting Zn in the wurtzite-type structure of ZnO. However, x-ray magnetic circular dichroism at the Co $L_{2,3}$ edges reveals that the Co $3d$ sublattice is paramagnetic at all temperatures down to 2 K, both at the surface and in the bulk of the films. The Co $3d$ magnetic moment at room temperature is considerably smaller than that inferred from bulk magnetization measurements, suggesting that the Co $3d$ electrons are not directly at the origin of the observed ferromagnetism.

DOI: [10.1103/PhysRevB.76.125201](https://doi.org/10.1103/PhysRevB.76.125201)

PACS number(s): 75.50.Pp, 61.10.Ht, 75.30.Hx, 75.50.Dd

Among the most investigated topics in the field of spin electronics, dilute magnetic semiconductors (DMSs) occupy a prominent position, because they would allow one to exploit efficiently the spin and the charge of the electrons in the same device. In fact, electronic devices have been working for decades omitting the spin of the electron. In 1990, Datta and Das proposed a new magnetoelectronic device (a field effect transistor),¹ whose practical realization has been hindered by the weak spin injection efficiency from a ferromagnet to a semiconductor. A ferromagnetic semiconductor would constitute, therefore, an alternative route toward the efficient spin injection into normal semiconductors. Until very recently, however, the main concern was related to the low Curie temperature of the known DMSs, which is well below room temperature and precludes, therefore, potential applications.² A significant breakthrough was achieved recently, since room temperature ferromagnetism was predicted³ and observed⁴⁻⁹ for semiconductors such as GaN and ZnO doped with Co, Mn, or other transition metals. However, many reports remain controversial and the nature of the magnetic coupling has not been revealed yet. In fact, the original prediction of high T_C ferromagnetism in these systems by Dietl *et al.*³ lies on the assumption that they can be properly doped with p -type carriers, which would mediate the magnetic interactions. However, in order to account for the numerous experimental observations of ferromagnetism in n -type ZnO, alternative models have been proposed, which mainly rely on the presence of defects (like, for example, vacancies or interstitials).^{10,11} In most of these models, the presence of a magnetic impurity such as Co or Mn is a necessary ingredient for the appearance of ferromagnetism, but other models show that this might not be needed and that ferromagnetism can appear also in undoped oxides.¹² To date, however, there has not been any clear experimental proof of the validity of any of these models and of the role of the magnetic dopants.

In order to tackle these problems, we have performed extensive studies by x-ray absorption spectroscopies of Co doped ZnO films, which are ferromagnetic above room temperature according to bulk magnetization studies. Our results show that, within the sensitivity limits of these techniques, Co substitutes for Zn in the wurtzite structure, which is typical for ZnO, and that the Co magnetic sublattice is paramagnetic, with strong antiferromagnetic correlations.

Films of $\text{Zn}_{1-x}\text{Co}_x\text{O}$ ($x=0.1$ and 0.25) were grown on $\text{Al}_2\text{O}_3(0001)$ substrates by reactive magnetron cosputtering using pure Zn and Co targets. The working pressure was a mixture of argon at 5×10^{-3} Torr and oxygen at 1.5×10^{-3} Torr. The thickness of the films was fixed at 100 nm and their composition was controlled by adjusting the sputtering power applied to the Co and Zn targets. During the deposition, the substrates were kept at 600 °C. The films are transparent, and standard x-ray diffraction experiments reveal that they are highly textured along the c axis of the hexagonal wurtzite structure (space group $P6_3mc$). The $\text{Zn}_{0.9}\text{Co}_{0.1}\text{O}$ film was additionally implanted with 0.5% As^+ ions in order to increase the number of free carriers. While $\text{Zn}_{0.75}\text{Co}_{0.25}\text{O}$ is clearly insulating (resistance of the order of megohms at room temperature), As implantation induces a considerable reduction of the electrical resistance at room temperature and Hall effect measurements indicate that the $\text{Zn}_{0.9}\text{Co}_{0.1}\text{O}:\text{As}$ film is n -doped with a carrier concentration of $\sim 2 \times 10^{19} \text{ cm}^{-3}$.¹³ The optical absorption spectra, as measured by UV-visible transmission spectroscopy at room temperature, show the absorption bands which are characteristic of $d-d$ transitions in tetrahedrally coordinated high spin Co^{2+} (at wavelengths $\lambda \sim 570, 615, \text{ and } 655 \text{ nm}$), thus suggesting that Co substitutes for Zn in the wurtzite structure of ZnO.^{13,14} Moreover, a clear shift of the absorption edge toward higher wavelengths is observed as the Co concentration increases. The structural, optical, and electrical properties of

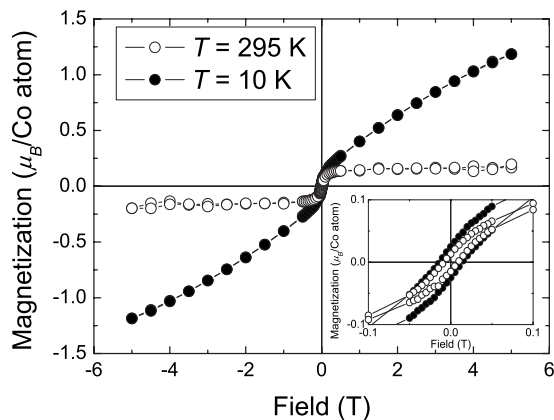


FIG. 1. Magnetization curves measured by SQUID magnetometry at different temperatures on $\text{Zn}_{0.9}\text{Co}_{0.1}\text{O}:\text{As}$ thin films, after subtraction of the diamagnetic contribution of the Al_2O_3 substrate. The magnetic field was applied perpendicular to the crystallographic c axis (i.e., parallel to the film's surface). The inset shows a zoom of the region of low magnetic fields that evidences the presence of a hysteresis.

these films have already been discussed in detail in Refs. 13 and 14.

The bulk magnetic properties of the $\text{Zn}_{1-x}\text{Co}_x\text{O}$ films were studied by superconducting quantum interference device (SQUID) magnetometry in the temperature range between 5 and 295 K in magnetic fields up to 5 T. Figure 1 shows the magnetization curves of $\text{Zn}_{0.9}\text{Co}_{0.1}\text{O}:\text{As}$ measured at room temperature and at 10 K as a function of applied magnetic field, whose direction was perpendicular to the crystallographic c axis of the film. At 295 K, a hysteresis loop opens at small fields, with a coercive field of the order of 9 mT, and the magnetization shows little dependence on the magnetic field for fields larger than 0.5 T. These findings indicate that the film is ferromagnetic, with a Curie temperature higher than room temperature. The magnetization measured in a field of 10 mT shows little dependence on temperature between 295 and 50 K. However, below 50 K, the susceptibility increases sharply with decreasing temperature, thus indicating the presence of paramagnetic moments.¹³ This is confirmed by the field dependence of the magnetization measured at 10 K (see Fig. 1), which is the superposition of a ferromagnetic component (coercive field of ≈ 14 mT) and a paramagnetic component. Similar results were obtained on the $\text{Zn}_{0.75}\text{Co}_{0.25}\text{O}$ film, which additionally shows a clear magnetic anisotropy, with the magnetic moment along the c axis being greater (by a factor of ~ 2) than the moment in the film's plane (see Ref. 14).

Information about the structural and electronic properties of $\text{Zn}_{1-x}\text{Co}_x\text{O}$ was obtained by x-ray absorption spectroscopy (XAS) and x-ray natural linear dichroism (XNLD) at the K edges of Zn and Co ($1s \rightarrow 4p$ transitions), performed at beamline ID12 of the European Synchrotron Radiation Facility, Grenoble, France, at room temperature and in total fluorescence yield mode. The measurements were done by rotating the direction of the polarization vector \mathbf{E} with respect to the crystallographic c axis. Figures 2(a) and 2(b) show the polarization dependent XAS spectra of

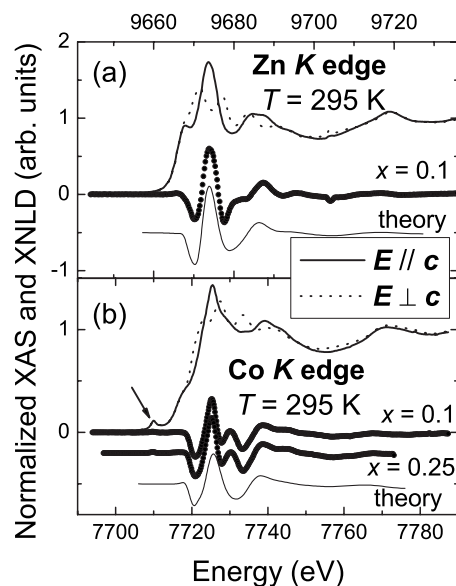


FIG. 2. The room temperature XAS spectra of $\text{Zn}_{0.9}\text{Co}_{0.1}\text{O}:\text{As}$ and $\text{Zn}_{0.75}\text{Co}_{0.25}\text{O}$ as measured at (a) the Zn and (b) the Co K edge, with the polarization vector of the x rays parallel (thick solid line) and perpendicular (thick dotted line) to the crystallographic c axis, and their difference (XNLD, full circles). The calculated XNLD is shown as a thin solid line and is shifted vertically for clarity, as well as the XNLD curve for $\text{Zn}_{0.75}\text{Co}_{0.25}\text{O}$ at the Co K edge.

$\text{Zn}_{0.9}\text{Co}_{0.1}\text{O}:\text{As}$ and $\text{Zn}_{0.75}\text{Co}_{0.25}\text{O}$ at the Zn and Co K edges. Identical results were obtained on other films with Co concentrations $0 \leq x \leq 0.25$. The strong anisotropy of the x-ray absorption at both K edges, due to the preferential growth of the films with the c axis perpendicular to the surface, leads to the observation of a strong XNLD signal. The K edge XAS spectra of $\text{Zn}_{1-x}\text{Co}_x\text{O}$ films have been calculated by using the *ab initio* code FDMNES,¹⁵ in the mode which uses the multiple scattering formalism on a muffin-tin potential. Figures 2(a) and 2(b) show a comparison of the experimental XNLD signals with those extracted from the *ab initio* calculations on a 77-atom cluster (6 Å radius). The Zn K edge XNLD can well be approximated by that of pure ZnO [as shown in Fig. 2(a)], thus confirming that the introduction of Co does not significantly change the structural properties of the ZnO matrix. Some small discrepancies between experiment and model are evident in the region just above the absorption edge and are due to the limited size of the cluster used in the calculations (which was chosen as a good compromise between accuracy of the calculation and computational time). The Co K edge XNLD has been calculated by artificially replacing all the Zn^{2+} ions by Co^{2+} ions in the wurtzite-type structure of ZnO (without any change in the lattice constants). Although this is an approximation, it can be considered as justified by the fact that the Co K edge XAS and XNLD spectra are the same for the whole range of Co concentrations between 5% and 25%. Even in this case the agreement between experiment and calculation is very good [see Fig. 2(b)], thus confirming that Co is occupying substitutional positions. It is especially important to note that the calculated XNLD signal has not been rescaled with respect to the experimental one, and this suggests that all Co atoms

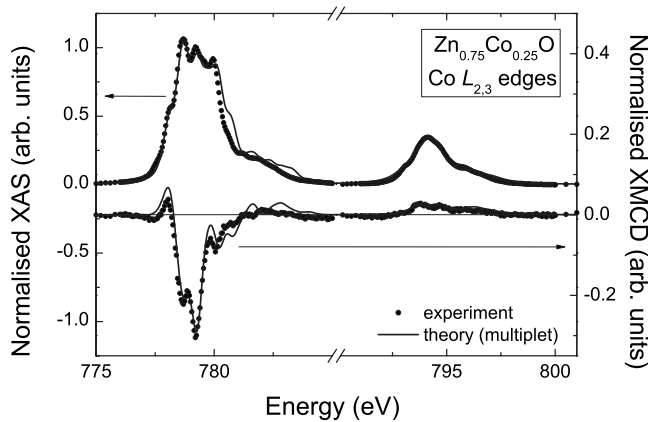


FIG. 3. Isotropic XAS and XMCD spectra measured (full circles, TEY) and calculated within the theory of atomic multiplets (thick solid lines) for $\text{Zn}_{0.75}\text{Co}_{0.25}\text{O}$ at the $\text{Co } L_{2,3}$ edges.

occupy positions with the same symmetry in the lattice. A small amount ($\leq 5\%$ of the total Co concentration) of clusters of metallic Co, for example, would not only have a visible influence on the shape of the XAS spectrum, but it would also reduce the measured XNLD amplitude (to which metallic Co does not contribute) with respect to the calculated one.

In order to investigate independently the magnetic properties of the Co sublattice, XAS and x-ray magnetic circular dichroism (XMCD) measurements at the $\text{Co } L_{2,3}$ edges ($2p \rightarrow 3d$ transitions) were performed at beamlines UE56/2 and UE46 of BESSY, Berlin, Germany ($\text{Zn}_{0.9}\text{Co}_{0.1}\text{O}:\text{As}$ film) and SIM of the Swiss Light Source, Villigen, Switzerland ($\text{Zn}_{0.75}\text{Co}_{0.25}\text{O}$ film). The XAS signal was detected simultaneously in both total electron yield (TEY) and total fluorescence yield (TFY) modes, ensuring both surface and bulk sensitivities, respectively. The XAS and XMCD spectra measured at the $\text{Co } L_{2,3}$ edges in TEY mode show a pronounced multiplet structure at both edges (see Fig. 3 for the case of $x=0.25$), which is typical for cobalt in a nonmetallic environment. These spectra are very similar to those reported for $\text{Zn}_{1-x}\text{Co}_x\text{O}$ films in Ref. 16. In order to simulate both XAS and XMCD spectra, multiplet calculations were performed with a program based on Cowan's Hartree-Fock atomic code with point charge crystal field.¹⁷ Figure 3 shows that an excellent agreement between experiment and theory can be achieved if we consider Co^{2+} ions ($3d^7$ configuration) occupying sites with C_{3v} point symmetry, as expected if Co substitutes for Zn. The crystal field parameters which best fit simultaneously both XAS and XMCD spectra are $10D_q = -0.47$ eV, $D\sigma = 0.06$ eV, and $D\tau = -0.03$ eV.

Element selective magnetization curves have been recorded in both TEY and TFY at 2, 5, and 25 K on $\text{Zn}_{0.9}\text{Co}_{0.1}\text{O}:\text{As}$ by scanning the magnetic field while keeping the incident energy fixed at the maximum of the XMCD signal at the $\text{Co } L_3$ edge ($E=779.2$ eV), at both normal and 45° incidence. The magnetic field, in all the XMCD measurements described in this paper, was applied in a direction parallel to the propagation direction of the x-ray beam: at normal incidence, the magnetic field is, therefore, applied

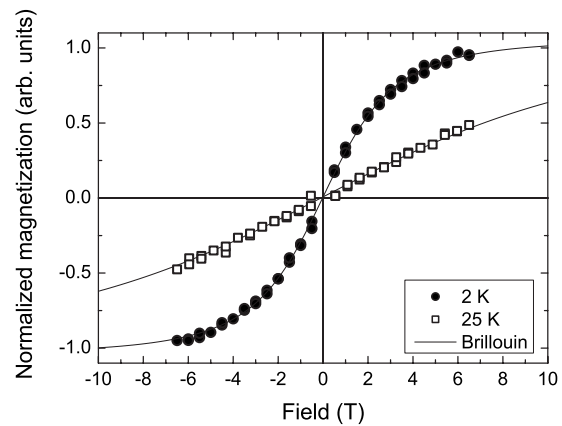


FIG. 4. Normalized magnetization curves of $\text{Zn}_{0.9}\text{Co}_{0.1}\text{O}:\text{As}$ measured at the $\text{Co } L_3$ edge in TEY at $T=2$ K (full circles) and at $T=25$ K (empty squares). The magnetization curves are compared with Brillouin functions calculated for $S=3/2$ and $L/S=0.7$ (solid lines).

perpendicular to the film's surface, while at 45° incidence, the magnetic field is applied at both 45° from the film's surface and 45° from the film's c axis. Figure 4 shows as an example the curves measured in TEY at 2 and 25 K at 45° incidence, which are normalized to a saturation magnetization of 1. In this geometry, the measurements are sensitive to both the in-plane and out-of-plane magnetizations. Although these measurements do not give directly an absolute value of the Co magnetic moment as a function of the applied magnetic field, they give a first clear indication about the field dependence of the magnetization of Co in $\text{Zn}_{0.9}\text{Co}_{0.1}\text{O}:\text{As}$. The curves measured at all temperatures can well be accounted for by Brillouin functions (shown as continuous lines in the figure), calculated with the fixed values of $S=3/2$ (for Co^{2+}) and $L/S=0.7$ (this value of L/S is determined through the application of the magneto-optical sum rules to the XAS and XMCD spectra as discussed below). Strikingly and unexpectedly, the results displayed in Fig. 4 show, therefore, the presence of a purely paramagnetic contribution of the $\text{Co } 3d$ sublattice to the total magnetization of the $\text{Zn}_{0.9}\text{Co}_{0.1}\text{O}:\text{As}$ film. This paramagnetic behavior is confirmed by the absence of any detectable hysteresis in the magnetization curves measured by XMCD, both at normal and 45° incidence. Similar results were obtained in TFY mode, so that we cannot observe any difference in the magnetic properties of the surface (measurements in TEY mode) and of the bulk (measurements in TFY mode), as well as on the $\text{Zn}_{0.75}\text{Co}_{0.25}\text{O}$ film.

More quantitative information can be obtained by the application of the magneto-optical sum rules, which allow one to evaluate separately both the spin and the orbital magnetic moments carried by the Co atoms.^{18,19} We suppose a pure $3d^7$ configuration for the Co atoms (in agreement with the multiplet and the *ab initio* calculations of the XAS spectra), which fixes the number of holes in the $3d$ shell to 3. In this case, we obtain for $\text{Zn}_{0.9}\text{Co}_{0.1}\text{O}:\text{As}$ a spin magnetic moment $m_S=0.81(8)\mu_B$ and an orbital magnetic moment $m_L=0.27(3)\mu_B$ at $T=2$ K and $H=6.5$ T in normal incidence and TEY. Slightly larger values [$m_S=0.97(10)\mu_B$ and m_L

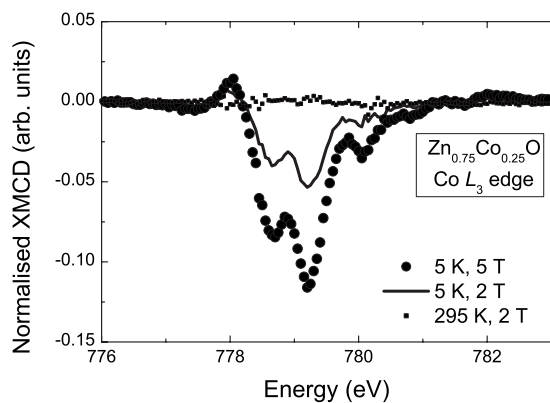


FIG. 5. Zoom of the XMCD spectra of $\text{Zn}_{0.75}\text{Co}_{0.25}\text{O}$ measured at the $\text{Co } L_3$ edge in TEY at $T=5$ K and $H=5$ T (full circles), at $T=5$ K and $H=2$ T (continuous lines), and at $T=295$ K and $H=2$ T (small full squares).

$=0.31(3)\mu_B$] are obtained at 45° incidence (TEY), suggesting the presence of a small anisotropy of the $3d$ magnetic moment. However, the ratio m_L/m_S keeps a constant value of $\sim 0.35(4)$. The total magnetic moment $m_{\text{tot}} \approx 1.2(1)\mu_B$ is considerably lower than the value of $\sim 4\mu_B$, which would be expected for $S=3/2$ and for the value $L/S=2m_L/m_S \sim 0.7$ determined experimentally from the application of the sum rules. Similar results were obtained on $\text{Zn}_{0.75}\text{Co}_{0.25}\text{O}$ (see Fig. 5), but with an even more reduced magnetic moment of $m_{\text{tot}}=0.55(6)\mu_B/\text{Co}$ atom at 5 K and 5 T, measured in TEY mode and normal incidence. This reduction of the total magnetization has already been observed in most bulk $\text{Zn}_{1-x}\text{Co}_x\text{O}$ samples with large Co concentrations and has been attributed to an inhomogeneous distribution of the Co atoms in the ZnO lattice.^{20,21} This gives rise to strong local Co-Co antiferromagnetic correlations, mediated by neighboring O atoms, and can possibly lead to the onset of antiferromagnetic order in the Co rich regions, which would, therefore, not contribute to the total magnetization. We can tentatively ascribe to this mechanism the observation of a low saturation magnetization of the Co sublattice in our samples as well as the lower total magnetic moment of $\text{Zn}_{0.75}\text{Co}_{0.25}\text{O}$ as compared to $\text{Zn}_{0.9}\text{Co}_{0.1}\text{O}:\text{As}$.

The total Co magnetic moment in $\text{Zn}_{0.9}\text{Co}_{0.1}\text{O}:\text{As}$ decreases rapidly with increasing temperature [$m_{\text{tot}}=0.65(7)\mu_B$ at $T=25$ K and $H=6.5$ T] and almost vanishes at room temperature, where $m_{\text{tot}}=0.05(3)\mu_B$ at $H=4$ T. A similar trend is observed in the case of $\text{Zn}_{0.75}\text{Co}_{0.25}\text{O}$ (see Fig. 5), where the XMCD at $H=2$ T and $T=295$ K falls below the detection limit, indicating that the Co magnetic moment is well below $0.01\mu_B$. This is in stark contrast with the result of the bulk magnetization measurements, which show a ferromagnetic signal at least four times larger under the same conditions (see Fig. 1 and Ref. 14). The XAS and XMCD spectra measured in TFY mode are qualitatively similar, but the strong self-absorption in the sample alters significantly the branching ratio between the L_2 and L_3 absorption edges, thus making the application of the sum rules meaningless. However, they qualitatively confirm the strong decrease of the total Co magnetic moment with increasing temperature also in the bulk of the sample.

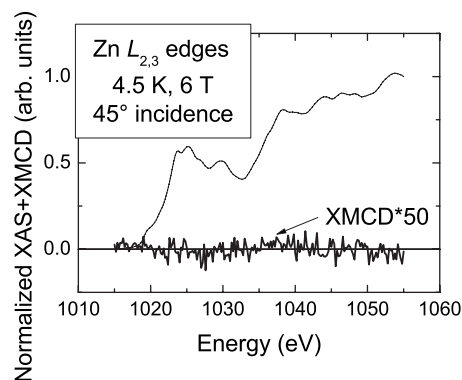


FIG. 6. The XAS spectra of $\text{Zn}_{0.9}\text{Co}_{0.1}\text{O}:\text{As}$ measured at the $\text{Zn } L_{2,3}$ edges in TFY mode, 45° incidence, $T=4.5$ K, and $H=6$ T, with right circularly polarized (thin solid line) and left circularly polarized (thin dotted line) x rays, and the corresponding XMCD spectrum (thick solid line).

All these findings are in stark contrast with the results of the bulk magnetization measurements and strongly support the idea that the Co doping is not the primary cause of the high temperature ferromagnetism observed in the $\text{Zn}_{1-x}\text{Co}_x\text{O}$ films. The paramagnetic contribution to the bulk magnetization, as obtained by subtracting the magnetization measured at 295 K from that at 10 K, amounts to $m_{\text{par}}=1.0(1)\mu_B/\text{Co}$ atom at 5 T and 10 K for $\text{Zn}_{0.9}\text{Co}_{0.1}\text{O}:\text{As}$ and coincides, therefore, within the error, with the total Co $3d$ magnetic moment determined by the XMCD measurements. These findings allow us to attribute all the paramagnetic signal to the $3d$ moments of the Co sublattice and, at the same time, to exclude their significant contribution to the ferromagnetism. We cannot, however, exclude the presence of a tiny ferromagnetic Co $3d$ moment (as expected in the case of long range ferromagnetic order), below the detection limit of our XMCD measurements ($\sim 0.01\mu_B$), but this would be much lower than the ferromagnetic moment measured by SQUID magnetometry at room temperature.

In order to further investigate the origin of ferromagnetism in our $\text{Zn}_{0.9}\text{Co}_{0.1}\text{O}:\text{As}$ film, we searched for the possible magnetic polarization of the Zn sublattice. The electronic configuration for Zn^{2+} is formally $3d^{10}$, so that a $3d$ magnetic moment cannot be expected to be present. However, the presence of vacancies and/or interstitial Zn atoms could be at the origin of an unfilled $3d$ shell, which could, in turn, carry a magnetic moment. Figure 6 shows the XAS and XMCD spectra measured in TFY at the $\text{Zn } L_{2,3}$ edges at $T=4.5$ K and $H=6$ T. The XAS spectra do not show the presence of any strong white line, as expected for a fairly pure $3d^{10}$ configuration. There is no evidence of an XMCD signal in the measured energy region, down to the noise level of 0.15% of the jump at the edge. This excludes the presence of any detectable ferromagnetic polarization of the Zn s and d shells.

These results indicate, therefore, that the $3d$ electronic shells of the cations in our $\text{Zn}_{1-x}\text{Co}_x\text{O}$ films do not carry any measurable ferromagnetic moment, contrary to what is usually assumed in the theoretical models proposed to account for the unexpected magnetic properties of this and related

systems. This seems to suggest that mostly the anion sublattice (i.e., the oxygen ions) might be responsible for the ferromagnetic moment observed in $\text{Zn}_{1-x}\text{Co}_x\text{O}$ (for example, through the presence of vacancies or interstitials) and that this and other doped oxides might exhibit properties similar to those of pure HfO_2 (Ref. 22) or TiO_2 (Ref. 23). Future investigations should, therefore, also be directed toward obtaining reliable XMCD signals at the O K edge in such systems.

In summary, we have investigated the structural and magnetic properties of films of $\text{Zn}_{1-x}\text{Co}_x\text{O}$ produced by reactive magnetron cosputtering. They show ferromagnetism with a Curie temperature T_C above room temperature in bulk magnetization measurements. At temperatures below ~ 50 K, a clear paramagnetic component appears, which dominates at the lowest temperatures. Our x-ray absorption measurements at the Co and Zn K and $L_{2,3}$ edges show that the Co atoms are in a divalent state and in tetrahedral coordination, thus substituting Zn in the wurtzite-type structure of ZnO. X-ray magnetic circular dichroism at the Co $L_{2,3}$ edges reveals that the Co sublattice is paramagnetic at all temperatures down to 2 K, both at the surface and in the bulk of the films. A total magnetic moment of $\sim 1.2\mu_B/\text{Co}$ atom is observed at 2 K

and 6.5 T for $\text{Zn}_{0.9}\text{Co}_{0.1}\text{O}$: As, of the same order as the paramagnetic contribution measured under similar conditions by SQUID magnetometry, but it is reduced to $\sim 0.55\mu_B/\text{Co}$ atom in $\text{Zn}_{0.75}\text{Co}_{0.25}\text{O}$ at 5 K and 5 T. No x-ray magnetic circular dichroism signal could be detected at the Zn $L_{2,3}$ edges, thus excluding the presence of a large magnetic polarization of the Zn sublattice. The ferromagnetic component observed by bulk magnetization up to room temperature cannot, therefore, be ascribed to the Co and Zn sublattices.

The authors would like to thank B. Muller, F. Maingot, A. Derory, and B. Zada for technical assistance, and R. Gusmeroli and C. Dallera for making their multiplet calculations software available and for their continuous assistance in performing the calculations. A.B. acknowledges fruitful discussions with N. Hoa Hong and D. Testemale. Work at Bessy was supported by the European Community-Research Infrastructure Action under the FP6 “Structuring the European Research Area” program (through the Integrated Infrastructure Initiative “Integrating Activity on Synchrotron and Free Electron Laser Science”-Contract No. R II 3-CT-2004-506008). Part of the work was performed at the Swiss Light Source, Paul Scherrer Institut, Villigen, Switzerland.

*Present address: CELLS-ALBA, Edifici Cn.-Módul C/3 Campus UAB, E-08193 Bellaterra, Barcelona, Spain; abarla@cells.es

- ¹S. Datta and B. Das, *Appl. Phys. Lett.* **56**, 665 (1990).
- ²K. W. Edmonds, K. Y. Wang, R. P. Campion, A. C. Neumann, N. R. S. Farley, B. L. Gallagher, and C. T. Foxon, *Appl. Phys. Lett.* **81**, 4991 (2002).
- ³T. Dietl, H. Ohno, F. Matsukura, J. Cibert, and D. Ferrand, *Science* **287**, 1019 (2000).
- ⁴For a recent review, see T. Fukumura, H. Toyosaki, and Y. Yamada, *Semicond. Sci. Technol.* **20**, S103 (2005).
- ⁵M. Venkatesan, C. B. Fitzgerald, J. G. Lunney, and J. M. D. Coey, *Phys. Rev. Lett.* **93**, 177206 (2004).
- ⁶K. R. Kittilstved, N. S. Norberg, and D. R. Gamelin, *Phys. Rev. Lett.* **94**, 147209 (2005).
- ⁷P. Sati *et al.*, *Phys. Rev. Lett.* **96**, 017203 (2006).
- ⁸G. T. Thaler *et al.*, *Appl. Phys. Lett.* **80**, 3964 (2002).
- ⁹K. Ando, *Appl. Phys. Lett.* **82**, 100 (2003).
- ¹⁰J. M. D. Coey, M. Venkatesan, and C. B. Fitzgerald, *Nature Mater.* **4**, 173 (2005).
- ¹¹C. H. Park and D. J. Chadi, *Phys. Rev. Lett.* **94**, 127204 (2005).
- ¹²I. S. Elfimov, S. Yunoki, and G. A. Sawatzky, *Phys. Rev. Lett.* **89**, 216403 (2002).

- ¹³H. Ndilimabaka, S. Colis, G. Schmerber, D. Müller, J. J. Grob, L. Gravier, C. Jan, E. Beaurepaire, and A. Dinia, *Chem. Phys. Lett.* **421**, 184 (2006).
- ¹⁴A. Dinia, G. Schmerber, C. Mény, V. Pierron-Bohnes, and E. Beaurepaire, *J. Appl. Phys.* **97**, 123908 (2005).
- ¹⁵Y. Joly, *Phys. Rev. B* **63**, 125120 (2001).
- ¹⁶M. Kobayashi *et al.*, *Phys. Rev. B* **72**, 201201(R) (2005).
- ¹⁷R. D. Cowan, *The Theory of Atomic Structure and Spectra* (University of California Press, Berkeley, 1981).
- ¹⁸B. T. Thole, P. Carra, F. Sette, and G. van der Laan, *Phys. Rev. Lett.* **68**, 1943 (1992).
- ¹⁹P. Carra, B. T. Thole, M. Altarelli, and X. Wang, *Phys. Rev. Lett.* **70**, 694 (1993).
- ²⁰M. Bouloudenine, N. Viart, S. Colis, J. Kortus, and A. Dinia, *Appl. Phys. Lett.* **87**, 052501 (2005).
- ²¹A. S. Risbud, N. A. Spaldin, Z. Q. Chen, S. Stemmer, and R. Seshadri, *Phys. Rev. B* **68**, 205202 (2003).
- ²²M. Venkatesan, C. B. Fitzgerald, and J. M. D. Coey, *Nature (London)* **430**, 630 (2004).
- ²³N. H. Hong, J. Sakai, N. Poirot, and V. Brizé, *Phys. Rev. B* **73**, 132404 (2006).